Hydrological pulses and burning of dissolved organic carbon by stream respiration

Benoît O.L. Demars[1,2]

[1] Norwegian Institute for Water Research (NIVA), Gaustaallen 21, 0349 Oslo, Norway

[2] The James Hutton Institute, Craigiebuckler, Aberdeen AB15 8QH, UK

Tel. : +47 98 227 757

E-mail : benoit.demars@niva.no

Running header: Hydrological pulses and stream respiration

Abstract

Stream metabolism plays a significant role in the global carbon cycle. Storm events can lower stream metabolic activities by removing standing biomass and river bed stock of organic matter. However hydrological events could also stimulate stream ecosystem respiration by providing dissolved organic carbon derived from soils. Here I show how hydrological connectivity between land and water affects fluxes of dissolved organic carbon (DOC) and daily whole stream bacterial respiration over an annual cycle in streams rich in DOC in north-west Europe. The novelty of the approach resides in combining continuous whole stream metabolism with hydrological flow paths and water chemistry to quantify the *in-situ* fate of DOC at ecosystem scale, with an estimation of all major stream carbon fluxes (land derived CO_2, in-stream biotic CO_2, HCO_3 and DOC) at catchment scale. An average 23±11% of the annual dissolved organic carbon inputs from the land was respired away by benthic microbial metabolism within about an hour of transit time in small watersheds (about 1 km^2).

Stream ecosystem respiration was highly related to discharge and was stimulated for as long as the hydrological connectivity between land and water remained, as indicated by soil moisture continuous monitoring. In-stream heterotrophic respiration represented 16 ±7% of the annual total carbon fluxes (also including HCO_3, land derived CO_2, DOC) at the catchment outlet under stable flows. This study suggests that dissolved organic carbon supply (soil carbon loss) will increase with rainfall, stimulating aquatic respiration and CO_2 emissions in streams.

Keywords: stream metabolism method, dissolved organic matter, gas exchange, carbon cycling, hydrological flow paths

Introduction

Streams and rivers play a major role in the global carbon cycle (e.g. Cole et al. 2007; Battin et al. 2009; Raymond et al. 2013; Drake et al. 2018), also affecting carbon processes in downstream ecosystems (Bauer et al 2013). Our ability to make predictions under different scenarios of land use and climate change remains challenging however because of the spatial heterogeneity and temporal dynamics of carbon cycling processes across scales at the interfaces of land, water and atmosphere. The metabolic balance of streams plays a significant role in CO_2 emissions (e.g. Borges et al. 2015; Hotchkiss et al. 2015). This metabolic balance may not change with warming when the streams are disconnected from the soil (summer low flows, Demars et al. 2016), but the metabolic balance could be strongly affected by changes in carbon supply brought by hydrological pulses (Ulseth et al. 2018). In fact, carbon cycling in streams may be more affected by changes in hydrology than warming (Acuña and Tockner 2010).

Hydrological disturbances can flush downstream significant proportions of in-stream standing biomass and stock of organic matter (e.g. fine particulate organic matter, leaf packs), notably in rivers with mobile sediment. This led to testing the resistance and resilience concept of stream metabolism following hydrological events (e.g. Uehlinger 2000; Uehlinger 2006; Reisinger et al. 2017). Hydrological pulses also deliver dissolved organic carbon (DOC) to the stream from the land (e.g. Cooper et al 2007; Stutter et al. 2012; Fasching et al. 2016). While most of the DOC entering headwaters is transported downstream during peak flows in the river network (pulse-shunt concept, Raymond et al. 2016), changes in hydrological flow paths can also bring together reactants facilitating biogeochemical processes (hot spot and hot moment concept, McClain et al. 2003; ecosystem control points concept, Bernhardt et al. 2017). Several studies have reported stimulation of ecosystem respiration immediately following hydrological pulses (e.g. Roberts et al 2007, Griffiths et al 2013, Roley et al 2014), but this inference did not consider the potential confounding effects of concurrent changes in dissolved oxygen in lateral inflows known to bias ecosystem respiration estimates (e.g. McCutchan et al. 1998; Hall and Tank 2005; McCutchan and Lewis 2006).

Headwaters are tightly connected to the land and it has long been recognised that the interface between groundwater (or soil water) and surface water is a control point of labile dissolved organic matter processing (e.g. Fiebig and Lock 1991; Findlay and Sobczak 1996; Fischer et al. 2002; Kaplan et al. 2008; Drake et al. 2015; Stegen et al. 2016; Einarsdottir et al. 2017). The *in-situ* timing of inputs and fate of dissolved organic matter in headwater streams remain largely unknown however (Hotchkiss et al. 2015; Stimson et al. 2017), and is of particular importance in the cool temperate and boreal moist climate regions draining catchment areas rich in soil organic carbon (Scharlemann et al. 2014) and particularly susceptible to climate change (e.g. Schneider et al. 2013).

Here I show how hydrological connectivity between land and water affects fluxes of dissolved organic carbon (DOC) and daily whole stream bacterial respiration over an annual cycle in streams rich in DOC in north-west Europe. The novelty of the approach resides in combining continuous

whole stream metabolism (see Bernhardt et al. 2018) with hydrology and water chemistry to quantify the *in-situ* fate of DOC at ecosystem scale, with an estimation of all major stream carbon fluxes (land derived CO_2, in-stream biotic CO_2, HCO_3 and DOC) at catchment scale. I made use of a long-term monitoring site of the UK Environmental Change Network and installed additional instrumentation, in an adjacent paired stream, for replication.

Methods

Study area

The study area was located in cool temperate moist climate, within the Glensaugh research station of the James Hutton Institute in north-east Scotland (Long 2° 33' W, Lat 57° 55' N) – see http://www.hutton.ac.uk/about/facilities/glensaugh. Annual average precipitation and evapotranspiration are 1040 mm and 300 mm, respectively. The geology is coarse Dalradian acid schist drifts. The top of the catchment area (> 400m) is dominated by deep (> 0.50 m) peat soils, whilst at lower altitudes freely drained peaty podzols (350-400 m) and freely-drained humus iron podzols (250-350 m) predominate. Peaty gleys occupy flatter areas bordering the streams. The catchment areas of the studied streams (Cairn Burn and Birnie Burn) are < 1 km^2 and lie within an elevation of 265-450 m. These two first order streams drain incised valleys of rounded hilltops and are fed by small surface water flushes. The streams are about 0.8-1.0 m wide in the studied sections and their channels significantly undercut the banks by 30-46% of stream width. The open width is therefore narrower than the stream bed and may constrain gas exchange and light availability for photosynthesis. The catchment is used for hill farming: mixed grazing of sheep and cattle. The vegetation cover is predominantly grass and heather with rushes growing in the flushes and bracken on the hill slope along the stream. The management of the land includes regular heather burning (10-12% of surface area yearly target). In the late 1970s and early 80s two areas covering 33 ha were improved (reseeded, limed and fertilized) as part of sheep grazing experiments (Hill Farming

98 Research Organisation 1983). Brown trout (*Salmo trutta fario*, Salmonidae) is present in both
99 streams. The water chemistry is characterised by relatively high concentrations of nitrate and
100 dissolved organic carbon, but low concentrations of soluble reactive phosphorus (Table 1). For
101 further information about land management, vegetation, soil, hydrology and hydrochemistry see Hill
102 Farming Research Organisation (1983), Miller and Hirst (1998), Dunn et al. (2006), Cooper et al.
103 (2007), Stutter et al. (2012).

104

105 ## Birnie Burn: the Environmental Change Network (ECN) stream

106 The ECN stream (Birnie Burn) is part of the long-term monitoring of the UK Environmental Change
107 Network (ECN, http://data.ecn.ac.uk/), Fig. 1 and Fig. S1. The catchment has a fully automated
108 weather station on top of the hill (see above web links). Soil temperature and moisture are
109 monitored on the hillslope of the Birnie Burn at 275 m elevation (Cooper et al. 2007). Volumetric soil
110 moisture content is recorded every 30 minutes with Delta-T Devices ML2x ThetaProbes connected to
111 a Campbell Scientific CR10 datalogger. Monitoring depths of 10 and 45 cm, correspond respectively
112 to the base of the O (organic layer) and B (subsoil) horizons of the humus iron podzol present. The
113 soil solution is sampled every two weeks with replicated suction lysimeters at the same depths
114 (Prenart collectors). The stream is equipped with a flume for continuous monitoring of discharge
115 (catchment area 0.76 km^2) and dip water samples are collected weekly. Soil solution and water
116 samples are analysed for DOC, pH, nutrients (N, P) and major ions. – see Cooper et al. 2007 and
117 Stutter et al. 2012 for further details. Long term monitoring showed a substantial increase in annual
118 stream water DOC (flow weighted concentration increased by +0.28 mg C L^{-1} $year^{-1}$ during 1994-
119 2007, Stutter et al. 2011).

120

121 ## Cairn Burn: the paired stream

The ECN stream was paired with a neighbouring stream (Cairn Burn) in 2005. Samples were collected every week or two for stream water quality, see Fig. 1 and Fig. S1. The added facilities at the Cairn Burn (catchment area 0.9 km^2) included a 30.5 cm V-notch glass-fibre pre-calibrated flume ($Q=1.1028\ z^{2.12}$, with Q discharge in $m^3\ s^{-1}$ and z flume water depth in metre; Halcyon Solutions, Surrey, UK) and Campbell Scientific instruments (Loughborough, UK): water level with a sonic ranging sensor (SR 50) mounted on scaffolding, water electric conductivity and temperature probe (sensor CS547A with A547 interface), air temperature (thermistor with radiation shield) and barometric pressure (sensor RPT410F). Data were recorded every 5 minutes (Campbell Scientific CR10x datalogger) powered with a 12 V DC acid lead battery (PS100E), recharged with a 10 W solar panel (SP10). Data logger, battery and barometric pressure were housed in a weather resistant enclosure (ENC 12/14 GRP). Photosynthetic active radiations (PAR) were also recorded in air, one metre above ground, and at the same time step (LICOR LI-192 quantum sensor with LICOR LI-1400 data logger, Lincoln, NE, USA).

Terrestrial DOC: main source of organic carbon

Several studies in the above catchments suggested mechanistic links between soil porewater DOC and stream DOC (e.g. Cooper et al. 2007; Stutter et al. 2012) and pointed out the key role played by hydrology in top soil DOC flux (Buckingham et al. 2008). The two streams are also adjacent to a comparable catchment (Glen Dye) in which several studies on carbon cycling and carbon source partitioning have been made, notably Brocky Burn, a sub-catchment with similar size and properties (e.g. Hope et al. 2001; Palmer et al. 2001; Dawson et al. 2002; 2004). Dawson et al. 2002; 2004 showed DOC was the dominant flux of C via stream network. This DOC was of terrestrial origin as shown by $\delta^{13}C$ analyses of the natural DOC against terrestrial and aquatic plant material (Stutter et al. 2013). The concentration of particulate organic carbon (POC) in the Cairn Burn was very low and averaged (±sem) 0.19±0.03 mg L^{-1} (18 samples collected at regular intervals from March 2005 to May

147 2007, within a discharge range of 3-76 L s^{-1}, Marc Stutter, unpublished data). This was only 2% of the
148 organic carbon concentration, with DOC representing 98% (9.3±1.7 mg L^{-1}). The POC fraction was
149 therefore even lower than for the Brocky Burn (Dawson et al 2002) and was considered insignificant
150 in the present study. Chlorophyll a concentration in the water column was extremely low (< 1 µg L^{-1},
151 Stutter et al. 2013). These streams also have a small pool of sediment fine POC with an average
152 carbon content of the sediment fine fraction (<2 mm) of only 2.2±0.8 % based on a spatial survey of
153 26 comparable streams in the River Spey catchment (Demars and Edwards 2007). In the Cairn and
154 Birnie Burn the standing mass of coarse POC was < 10 g C m^{-2} (Demars, unpublished).

155

156

157 ## Whole stream metabolism

158 Whole stream metabolism was estimated with the open channel two-station diel oxygen method of
159 Odum (1956) modified by Demars et al. 2011b; 2015; 2017 and further improved below. The net
160 metabolism was previously calculated as follows (Demars et al. 2011b):

161 $$NEP_t = \left(C_{AV\,t+\tau} - C_{AV\,t} - k_2\tau(C_s - C_{AV\,t})\right)\frac{Q}{wL} - \left(C_g - C_{AV\,t}\right)\frac{Q_g}{wL}$$

162 with NEP_t net ecosystem production at time t (g O_2 m^{-2} min^{-1}), C_{AV} average dissolved oxygen (g O_2 m^{-3}) of the two stations at time $t+\tau$ and t (min), τ mean travel time (min), k_2 oxygen exchange coefficient (min^{-1}), C_s saturated oxygen concentration (g O_2 m^{-3}), Q discharge (m^3 min^{-1}), w average stream width (m), L reach length (m), C_g oxygen concentration in lateral inflows (g O_2 m^{-3}), and Q_g lateral inflows (m^3 min^{-1}). The second part of the equation is a correction for lateral inflows according to Hall and Tank (2005), see below for parameter estimation. Mathematically, the equation can also be solved for a fixed time interval. We have, after factoring,

169 $$NEP_t = \left(C_{AV\,t+\tau} - C_{AV\,t} - k_2\tau(C_s - C_{AV\,t}) - \theta\left(C_g - C_{AV\,t}\right)\right)\frac{Q}{wL}$$

with $\theta = Q_g/Q$, the proportion of lateral inflows. Since we have

$$u = \frac{L}{\tau}, we\ have \frac{Q}{wL} = \frac{uwz}{wL} = \frac{z}{\tau}$$

with z average depth (m), *u* average velocity (m min^{-1}) and τ mean travel time (min) between the two stations. Then we have:

$$NEP_t = \left(C_{AV\ t+\tau} - C_{AV\ t} - k_2\tau(C_s - C_{AV\ t}) - \theta\left(C_g - C_{AV\ t}\right)\right)\frac{z}{\tau}$$

$$NEP_t = \left(\frac{C_{AV\ t+\tau} - C_{AV\ t}}{\tau} - k_2(C_s - C_{AV\ t}) - \frac{\theta\left(C_g - C_{AV\ t}\right)}{\tau}\right)z$$

which is equivalent to

$$NEP_t = \left(\frac{C_{AV\ t+\Delta t} - C_{AV\ t}}{\Delta t} - k_2(C_s - C_{AV\ t}) - \frac{\theta\left(C_g - C_{AV\ t}\right)}{\Delta t}\right)z$$

with *Δt* time interval (min). This form of the equation is easier to use in long term studies because τ changes with discharge but *Δt* is a constant time interval. I used it in the present study with *Δt*=15 min.

Many tracer studies (NaCl, propane) were carried out as detailed in Demars et al. (2011b) to estimate lateral inflows, mean travel time and reaeration coefficient as a function of discharge within the range of stable flows (up to 32 L s^{-1}), well within the channel water conveyance capacity (>100 L s^{-1}). The relationships with discharge were very strong (R^2=0.88-0.95, Fig 2) allowing accurate parameterisation of metabolism calculations under varying flow conditions as e.g. Roberts et al. (2007) and Beaulieu et al. (2013). Oxygen concentrations were measured with optical sensors fitted on multiparameter sondes TROLL9500 Professional (In-Situ Inc., Ft Collins, CO, USA). Two sondes were deployed at 74 m interval in the Cairn Burn (138-212 m upstream of the flume). Another two sondes were set in the ECN stream Birnie Burn at 88 m interval (60-148 m upstream of the ECN flume). The distances between oxygen stations corresponded to 80-90% of the oxygen sensor footprints ($3u/k_2$), with u/k_2 entirely independent of discharge (R^2=0.0005). All sondes were

192 deployed from May to October 2007, logging at 5 min time step interval. Recording continued until
193 July 2008 for the paired reach of the Cairn Burn, with only one oxygen sensor at the bottom station
194 from March 2008. Two post processing filters were installed at the end of the stream metabolism
195 calculations to constrain the results within the range of flows for which the parameters were
196 estimated (travel time, reaeration coefficient, depth) and to focus on base flow conditions. First,
197 metabolic estimates were only reported for days with discharge up to 30 L s^{-1} in the Cairn Burn
198 (catching 82% of flow conditions) and 27.4 L s^{-1} in the Birnie Burn (86% of flow conditions). Second,
199 days with a discharge coefficient of variation above 25% were excluded. Some data were lost due to
200 logging issues (battery failure), high flow impacts (sondes buried under gravel, broken sondes),
201 detached algal mat trapped around the sensor, and sonde malfunction (drift and sudden step
202 change in dissolved oxygen for one sonde). Daily to weekly visits limited these issues and the one-
203 station method was used to calculate metabolism when oxygen data was only available for one
204 station. The daily data were inspected visually to check their quality.

205

206 *Corrections for lateral inflows*. The sites were chosen to minimise the effect of lateral inflows. The
207 proportion of lateral inflows relative to discharge (Q_g/Q) was 10.7% and 6.6% for the Birnie Burn and
208 Cairn Burn reach, respectively, independently of discharge in the range 3.8-32.5 L s^{-1} (stable flows).
209 Adequate corrections required the estimation of the proportion of flow from surface water (flushes),
210 groundwater and subsurface soil water and their respective concentrations. In practice this can be
211 achieved with an end member mixing analysis coupled to a spatially explicit hydrological model, but
212 the ion end members proved to be very difficult to characterise at Glensaugh due to spatial
213 catchment heterogeneity (Dunn et al. 2006; Stutter et al. 2012) and a stable isotope approach using
214 $\delta^{18}O$ was not conclusive (Dunn et al. 2008). The proportion of base flow may be estimated another
215 way, simply using the hydrograph (e.g. Brodie and Hostetler 2005), according to the Base Flow Index
216 (BFI) method of Gustard et al. (1992). This method applies to the flow of the whole catchment,

rather than a stream reach, but is assumed here to be a reasonable approach for first order streams shown to have similar hydrological behaviours along their lengths (Dunn et al. 2006). The index ranges from 0-1, with low values representing very flashy flows and high values groundwater fed streams. The BFI of both streams was 0.43, calculated with daily average flow data from 2007-2008, reflecting the flashy flow regime as previously noted (Dunn et al. 2006). In the process daily base flows (Q_B) are estimated, and relative to the measured daily average discharge (Q), provide the daily proportion of baseflow $p(Q_B)=Q_B/Q$. The proportion of baseflow $p(Q_B)$ can be expressed as a function of discharge (ln transformed to normalise the data) with a logistic regression:

$$p(Q_B) = 1/\left(1 + exp(a\ln(Q) - b)\right)$$

with a, b stream reach constants (pseudo R^2=0.68, Fig S2). I estimated C_g from the proportion of baseflow (groundwater and lateral open water flushes) as $p(Q_B)$ and soil subsurface water as $1-p(Q_B)$, which is a reasonable assumption within Q=3-30 L s^{-1} under stable flow conditions (which will exclude overland flows). I assumed baseflow dissolved oxygen to be 90% of the stream saturated oxygen concentration (similar to field observations from springs and flushes) and sub-surface soil water only 10% of the stream saturated oxygen concentration (to provide a conservative estimate of the effect of lateral inflows on in-stream dissolved oxygen). The equation for a given stream reach is:

$$C_g = \left(1/\left(1 + exp(a\ln(Q) - b)\right)0.9C_s\right) + \left(1 - 1/\left(1 + exp(a\ln(Q) - b)\right)0.1C_s\right)$$

Uncertainties. The high oxygen reaeration coefficient of the studied streams (0.05-0.24 min^{-1}) required very accurate dissolved O_2 data. The sensors were calibrated to within 1% dissolved oxygen saturation (DOsat) at 100% air saturation in a 20 L fish tank with continuous air bubbling, using a Rena 301 air pump (200 L $hour^{-1}$) and 20 cm^2 air stone producing macro-bubbles (diameter in the mm range). I did not observe supersaturation of O_2 in the fish tank as in Hall et al. (2016), with independent measures done with the Winkler method averaging 100±2%. The calibration was

241 regularly checked across sensors in the stream (generally to within 1% DOsat) and the Winkler
242 method (within 2% DOsat accuracy). Calibration checks were also performed for individual oxygen
243 sensors in 100% saturated air.
244 The overall uncertainties in daily stream metabolism, including cross-calibration errors, individual
245 parameter uncertainties, spatial heterogeneity (through the average of diel O_2 curves) and
246 correction for lateral inflows, were propagated through all the calculations using Monte Carlo
247 simulations, assuming individual errors were normally distributed. Briefly, I repeated 250 times the
248 daily integration of ER and GPP assuming measurement errors of oxygen sensors, temperature,
249 atmospheric pressure and discharge were constant over a day (as generally observed). I repeated
250 the random draws for every 5 min time steps for the rating curve parameters (travel time, gas
251 exchange, C_g) and average oxygen concentrations and temperatures of the top and bottom stations.
252 When only one station was available, I assumed a standard deviation of 0.1 mg O_2 L^{-1} and 0.2°C for
253 oxygen and temperature, respectively. The median of the 250 runs provided a numerical solution for
254 ER and GPP. The 2.5^{th} and 97.5^{th} centiles provided a 95% confidence interval. All calculations were
255 run in Excel using preformatted spreadsheets. Random draws were carried out with the inverse of
256 the normal cumulative distribution for a specified mean and standard deviation using the function
257 NORM.INV(RAND(),mean,standard deviation) and the calculations repeated automatically with Data
258 Table. An example Excel spreadsheet is provided in Supplementary Information.
259

260 ## Quantification of carbon fluxes

261 *Biotic CO_2 emissions*. These were simply calculated as the net ecosystem production (NEP), gross
262 primary production (GPP) plus ecosystem respiration (ER, a negative flux) expressed in g C m^{-2} day^{-1}.
263 Respiration and photosynthesis rates in oxygen were converted to carbon using a respiratory and
264 photosynthetic quotient of 1 (Williams and del Giorgio 2005; Cory et al. 2014).
265

266 *Heterotrophic respiration*. Bacterial respiration of DOC was calculated as heterotrophic respiration
267 (HR, a negative flux) from:

268 $$HR = ER + \alpha GPP \text{ with } \alpha = AR/GPP$$

269 with AR, autotrophic respiration and ER, ecosystem respiration, both negative fluxes (oxygen
270 consumption) and GPP, positive flux (producing oxygen). I arbitrarily partitioned ER into auto and
271 heterotrophic respiration with α=0.5 (see Demars et al. 2015; Demars et al. 2017) and calculated
272 uncertainties using α=0.2 and α=0.8.

273

274 *Allochthonous organic carbon*. The overall flux at the outlet of both streams was calculated as
275 instantaneous discharge times DOC concentration at the time of sample collection using the weekly
276 data from the long-term monitoring collected in 2007-2008 under low stable flows. The DOC flux
277 was then related to discharge for low stable flows (3 to 30 L s^{-1}; Cairn n=61, R^2=0.74; Birnie n=88,
278 R^2=0.83) and all data available (Cairn n=74, R^2=0.85; Birnie n=100, R^2=0.83) to provide daily
279 estimates (within the same range of flows).

280 The organic carbon uptake length (Sw_{OC}, in m) and mineralisation velocity ($v_{f\text{-}OC}$, in m day^{-1}) were
281 calculated as in previous studies (Newbold et al. 1982; Hall et al. 2016), here neglecting POC (see
282 above):

283 $$Sw_{OC} = \frac{Q \times [DOC]}{-HR \times w}$$

284 with [DOC] dissolved organic carbon concentration (g C m^{-3}), Q discharge (m^3 day^{-1}), HR
285 heterotrophic respiration (a negative flux expressed in g C m^{-2} day^{-1}) and w width (m), and

286 $$v_{f-OC} = \frac{-HR}{[DOC]}$$

287

With all fluxes expressed in g C m^{-2} day^{-1}, I estimated the organic carbon ecosystem efficiency as follows (Newbold et al. 1982):

$$\varepsilon_{OC} = \frac{respired\ carbon}{carbon\ input}$$

The DOC supply (carbon input) is not known but is equivalent to the DOC mineralised plus DOC flux at the outlet. The heterotrophic respiration (*HR*) of the two streams studied here represented the mineralisation of DOC supply (respired carbon). The organic carbon ecosystem efficiency was upscaled to catchment scale as follows:

$$\varepsilon_{OC} = \frac{-HR\ w\ L}{(-HR\ w\ L) + (Q \times [DOC]_{outlet})}$$

with Q discharge, $[DOC]_{outlet}$ concentration of DOC at the outlet of the catchment, average stream width w=0.5 ±0.1 m and length L=1000 ±200 m in the watersheds. Note the length and depth were difficult to assess because of the temporal variability in discharge and sections of channels can be entirely covered by soil and vegetation in the upper part of the catchment, draining deep peat. This method allowed us to estimate the magnitude of the carbon fluxes for the whole catchments. This was calculated for all days with low stable flows (Q <30 L s^{-1}) for which HR estimates were available (Cairn Burn: 255 daily estimates over 439 days, Birnie Burn: 126 daily estimates over 184 days). I integrated HR and DOC flux over 365 days for the Cairn Burn. Since monitoring data was available for 439 days I integrated over a 365-day moving window and took the average. I also integrated HR and DOC flux over the 184 days for which data were available in both streams. Uncertainties were propagated in quadrature as above, using only the numerator and second part of the denominator.

Alkalinity. Alkalinity was analysed weekly, as part of the long-term monitoring program, by titration at pH=4.5 (Standing Committee of Analysts 1981) and converted to Gran alkalinity by adding 31.6 µeq HCO_3 L^{-1} (Neal 1988). Bicarbonate concentration [HCO_3] was multiplied by discharge to calculate

311 the carbon flux. The flux of HCO_3 was then related to discharge within the range of low stable flows
312 to provide daily estimates (Cairn n=47, R^2=0.79; Birnie n=65, R^2=0.88).

313

314 *Total CO_2 emissions*. In the absence of direct measurements, the excess partial pressure of CO_2
315 (E*p*CO_2) of the streams was estimated from three measured parameters: pH, Gran alkalinity and
316 temperature (Neal et al. 1998, as applied in Demars et al. 2016 with atmospheric CO_2=384 ppm,
317 ftp://ftp.cmdl.noaa.gov/ccg/co2/trends/co2_annmean_mlo.txt). The parameters were collected as
318 part of the long-term monitoring in both streams. The uncertainties in pH were assessed as ±0.2
319 units from comparisons of laboratory and *in-situ* measurements and high frequency observations of
320 *in-situ* diel variability during summer low flows (15 min time step, period 2009-2012, CS1M11-L glass
321 bulb pH probe, Wedgewood Analytical). The measured $pH_{20°C}$ was relatively high 6.83-7.37, but the
322 range in Gran alkalinity was relatively low (116-544 µeq HCO_3 L^{-1}) and the range in DOC was
323 relatively high (264-1028 µmol L^{-1}) suggesting that the results have high uncertainties. The
324 uncertainties in pCO_2 are probably around ±50% (Hope et al. 1995; Abril et al. 2015). E*p*CO_2 is the
325 concentration of free CO_2 in the stream water (C_t at time *t*) relative to the atmospheric equilibrium
326 free CO_2 concentration (C_{SAT}):

327 $$EpCO_2 = C_t / C_{SAT}$$

328 C_{SAT} was calculated from published CO_2 solubility in pure water at equilibrium with atmospheric CO_2
329 in the temperature range 0-90°C (Carroll 1991) and Henry's law (Stumm and Morgan 1981; Butler
330 1982). C_t was calculated as $EpCO_2 \times C_{SAT}$. The flux of CO_2 (F_{CO_2} , g C m^{-2} day^{-1}) at the interface
331 between water and the atmosphere was calculated as for oxygen (Young and Huryn 1998):

332 $$F_{CO_2} = k_{CO_2}(C_{SAT} - C_t)\tau\frac{Q}{A}$$

333 with k_{CO_2} reaeration coefficient of CO_2 (day^{-1}), $C_{SAT} - C_t$ average saturation deficit (mg C L^{-1} or g C m^{-3}), τ mean travel time of the stream reach (day), Q average water discharge (m^3 day^{-1}), A surface

335 water area of the stream reach (m^2). The reaeration coefficients between CO_2 and O_2 was simply
336 related as follows (Demars et al. 2015):

337 $$k_{CO_2} = \frac{Dm_{CO_2}}{Dm_{O_2}} k_{O_2} = 0.81 \pm 0.01 \, k_{O_2}$$

338 based on the molecular diffusivity (*Dm*) of CO_2 and O_2 measured at three different temperatures
339 with the same method (Davidson and Cullen 1957). The coefficient 0.81 was independent of
340 temperature. This approach is a simplification of more complex gas transfer velocity models (see e.g.
341 Demars and Manson 2013) and is known to have additional uncertainties from stream dual tracer
342 gas studies (Hall and Madinger 2018).

343 The flux of CO_2 was then related to discharge within the range of low stable flows for which stream
344 metabolism was processed (Cairn n=47, R^2=0.81; Birnie n=65, R^2=0.77) to provide daily estimates.

345 I assumed that CO_2 efflux related to NEP and HR was degassed back to the atmosphere without
346 significant bicarbonate formation because the stream was clearly not at equilibrium (constant CO_2
347 supersaturation, see results) and the time to reach the carbonate equilibrium (20-200 s, Zhang et al.
348 1995) approached the average time spent by a CO_2 molecule in the stream before emission in the
349 atmosphere (300-1000 s, calculated from travel time and reaeration coefficient of CO_2).

350 I upscaled the CO_2 efflux to the full length of the streams, as for HR above, so that all carbon fluxes
351 were comparable (also with the land-atmosphere fluxes), acknowledging that spatial heterogeneity
352 introduces another (unquantified) source of uncertainties (e.g. Dawson et al. 2001; Dawson et al.
353 2002).

354

355 ## Statistics

356 When regression analyses were based on time series with daily (continuous metabolism) or weekly
357 data (long term monitoring), individual datapoints were not independent, and the *P* values were

derived with a random cyclic shift method using 999 Monte Carlo restricted permutations for time series (Besag and Clifford 1989, ter Braak 1990, ter Braak & Šmilauer 2012). The analyses were performed with Canoco 5 (ter Braak & Šmilauer 2012) but the method is also available in the R package 'permute' (Simpson 2016).

Results

Whole stream metabolism

Gross primary productivity (GPP) ranged from near zero in the winter to about 3-5 g O_2 m^{-2} day^{-1} (1.1-1.9 g C m^{-2} day^{-1}) in spring and summer (paired stream), Fig. 3. In the summer, the Birnie Burn seemed more limited by light than the Cairn Burn with a lower GPP_{MAX} and lower half saturation point (Fig S3). The most conspicuous feature of the time series was high rates of ecosystem respiration (ER) following peak flows, with ER reaching repeatedly -25 to -35 g O_2 m^{-2} day^{-1} (-9.4 to -13.1 g C m^{-2} day^{-1}, see Fig. 3). It took weeks following a peak flow for ecosystem respiration to slowly return to a lower stable rate at about -5 to -7 g O_2 m^{-2} day^{-1} (-1.9 to -2.6 g C m^{-2} day^{-1}), independently of the season. The same patterns were observed for the ECN stream with ER of -20 g O_2 m^{-2} day^{-1} (-7.5 g C m^{-2} day^{-1}), while GPP remained within 1-5 g O_2 m^{-2} day^{-1} (0.4-1.9 g C m^{-2} day^{-1}, Fig S4).

In the paired stream, average net ecosystem production (NEP) was -4.1 (range -1 to -12.5) g C m^{-2} day^{-1}. In the ECN stream, average NEP was -5.8 (range -1.5 to -15.9) g C m^{-2} day^{-1}. In the paired stream, average heterotrophic respiration (HR) was -4.4 (±0.2 with $0.2<\alpha<0.8$) g C m^{-2} day^{-1} and ranged from -1.6 to -12.6 g C m^{-2} day^{-1}. In the ECN stream, average HR was -2.4 (range -0.9 to -6.4) g C m^{-2} day^{-1}. GPP did not influence much NEP or HR, both following the same dynamics as ER, highly related to discharge (Fig 4).

The numerical solutions of daily ER (ER_{NUM}) and GPP (GPP_{NUM}) using Monte Carlo simulations were very closely related to the deterministic results presented above for the Cairn Burn (ER_{NUM} =

382 1.11±0.002 ER + 0.84±0.04, R^2=0.998; GPP_{NUM} = 1.04 GPP - 0.02, R^2=0.991). The 95% confidence
383 interval was about 30% of ER_{NUM} – see Fig. 5. GPP uncertainties were more heterogenous likely
384 because most estimates were close to the limit of detection. GPP_{NUM} had one negative outlier for the
385 Cairn Burn, although it was not significantly different from zero (-0.45 g O_2 m^{-2} day^{-1}; 95% confidence
386 interval -1.08 to 0.07 g O_2 m^{-2} day^{-1}). The Birnie Burn had higher ER_{NUM} uncertainties (95% confidence
387 interval was about 50% of ER_{NUM}) but no negative GPP_{NUM} (Fig. S5). The numerical results were also
388 strongly related to the deterministic results, albeit with a noticeable bias for ER_{NUM} (ER_{NUM} =
389 1.27±0.01 ER + 1.98±0.11, R^2=0.985; GPP_{NUM} = 1.07±0.01 GPP - 0.22±0.03, R^2=0.956).

390

391 Carbon cycling and fluxes

392 *Carbon cycling*. The average organic carbon uptake lengths (Sw_{OC}) were 911 (range 286-2113) m and
393 2266 (range 841-4777) m; and the average mineralisation velocity ($v_{f\text{-}OC}$) were 1.24 (range 0.61-2.67)
394 m day^{-1} and 0.49 (0.21-1.09) m day^{-1} for the paired stream and ECN stream, respectively. The organic
395 carbon turnover length was only moderately related to discharge (Cairn: R^2=0.46, n=256, *P*=0.002,
396 Birnie: R^2=0.43, n=126, *P*=0.026). The mineralisation velocity was nearly entirely dependent on ER
397 (Cairn: R^2=0.92, *P*<0.001, Birnie: R^2=0.95, *P*<0.001).

398 *Carbon fluxes*. The DOC concentrations under low stable flows (Q<30 L s^{-1}) at the outlet of the
399 catchments were on average 4.0 (range 1.6-13.7) and 5.6 (range 3.2-12.3) mg C L^{-1} for the Cairn and
400 Birnie streams, respectively. DOC concentration was positively related to discharge (m^3 s^{-1}) in the
401 Cairn Burn (DOC = 18.4 $Q^{0.38}$, R^2=0.18, n=62, *P*=0.016) and Birnie Burn (DOC=18.8 $Q^{0.25}$, R^2=0.11,
402 n=89, *P*=0.008) during 2007-2008 under low stable flows (3 to 30 L s^{-1}). Similar relationships were
403 found using all available data with a wider range of flows (3-200 L s^{-1}): Cairn Burn (DOC = 19.0 $Q^{0.38}$,
404 R^2=0.30, n=74, *P*=0.006) and Birnie Burn (DOC = 20.5 $Q^{0.27}$, R^2=0.18, n=100, *P*=0.006) during the
405 same period. The average fluxes of DOC under low stable flows (3 to 30 L s^{-1}) at the outlet of the

406 catchments were 3800 (range 870-12700, Fig. 6) and 4300 (range 1400-15500, Fig. 6S) g C day^{-1} for
407 the Cairn and Birnie Burn, respectively.

408 The annual proportion of respired DOC (HR scaled up to the stream length of the catchments)
409 relative to the total DOC inputs (organic carbon ecosystem efficiency, ε_{OC}) was 36±18% for the paired
410 stream Cairn Burn under stable flow conditions (Fig 6). Varying the proportion of autotrophic
411 respiration from 0.2 to 0.8 in the calculation of HR did not introduce much uncertainties in our
412 results (35< ε_{OC} <37%). The organic carbon ecosystem efficiency for the ECN stream was 22±10%
413 from 1 May 2007 to 31 October 2007 under stable flow conditions (Fig S6); for comparison it was
414 31±15% for the same period for the paired stream.

415 The annual average heterotrophic respiration (HR) and DOC flux per unit area of land were 0.9±0.4
416 and 1.7±0.4 g C m^{-2} $year^{-1}$, respectively, under low flows (Cairn Burn data). Together these fluxes
417 represented 67±16% of the total DOC flux including all flow events (3.9±0.6 g C m^{-2} $year^{-1}$) during the
418 same period. Hence, 23±11% of the measured annual total flux of DOC at the outlet of a first order
419 stream has been respired away (assuming average HR under low flows is representative of HR under
420 high flows).

421 The excess partial pressure of CO_2 ($Ep CO_2$) at the outlet of the ECN stream was always above the
422 atmospheric pressure, even after accounting for uncertainties in measurements and diel changes
423 (0.2 pH unit). $Ep CO_2$ averaged 3.6 (2.2-5.6) with a minimum of 2.3 (1.4-3.6) and maximum of 5.6 (3.5-
424 8.8) times the atmospheric pressure. Similar $Ep CO_2$ were calculated for the paired stream: average
425 2.9 (1.8-4.6), minimum 1.8 (1.1-2.9), maximum 4.2(2.7-6.7) times the atmospheric pressure. Hence
426 both streams were continuously emitting CO_2 to the atmosphere. EpCO2 increased slightly with
427 discharge under low stable flows (3-30 L s^{-1}). The proportion of CO_2 efflux from HR (the
428 mineralisation of DOC) was particularly intense following peak flows and represented, an annual
429 average of 34±20 % of CO_2 emissions in the paired stream. For the period 1 May-31 October 2007,
430 the ECN stream released 37±21% of its CO_2 from HR (27±16% for the paired stream in the same

431 period). The average bicarbonate concentration was 270 (range 116-492) and 349 (range 147-544)
432 µmol HCO_3 L^{-1} based on Gran alkalinity, in the Cairn and Birnie Burn, respectively. While bicarbonate
433 concentrations decreased with discharge, the bicarbonate flux increased with discharge because the
434 relative change in bicarbonate was smaller than the relative change in discharge.

435 The above results allowed to compute the total C flux and its individual components (HR and land
436 derived CO_2, DOC, HCO_3) of both stream catchments under low flow conditions (Fig 7, Fig S7). The
437 annual carbon flux partitioning was as follows for the Cairn Burn (May 2007-July 2008): in-stream
438 heterotrophic respiration 16±7%, land derived CO_2 33±20%, HCO_3 22±7% and DOC 29±10%; and the
439 Birnie Burn (May 2007-October 2007): heterotrophic respiration 10±5%, land derived CO_2 28±20%,
440 HCO_3 25±10% and DOC 37±17%.

441

442 **Discussion**

443

444 Whole stream metabolism

445 Gross primary production (GPP) was similar to expectation for open streams (about 3 g O_2 m^{-2} day^{-1})
446 based on water temperature (Demars et al. 2016). The rates of ecosystem respiration (ER) following
447 peak flows were much greater (down to -20 to -35 g O_2 m^{-2} day^{-1}) however than what would be
448 expected at around 10°C (about -6 g O_2 m^{-2} day^{-1}). This was also in spite of low water stream
449 transient storage (cross sectional ratio As:A) under high discharge (0.2 at 30 L s^{-1} to 0.4 at 8 L s^{-1}) with
450 a residence time of water in the transient storage zone varying from 5 to 25 minutes (Manson et al.
451 2010), expecting ER to increase with transient storage (e.g. Battin et al. 2008; Demars et al. 2011a).
452 These high rates of ER resulted in NEP and HR rates of the same magnitude due to little GPP in the
453 two streams studied here. These high rates of ER were amongst the largest observed worldwide
454 from short term studies (Demars et al. 2016), and were similar to stream receiving industrial or

455 urban sewage (e.g. Izagirre et al. 2008). Such pulses in respiration rates following storm events have
456 been reported before (e.g. Roberts et al. 2007; O'Connor et al. 2012; Griffiths et al. 2013), but these
457 studies did not correct for the confounding effect of lateral inflows.

458 The numerical calculations of stream metabolism using Monte Carlo simulations improved the
459 propagation of errors from my previous attempts (Demars et al. 2011b; Demars et al. 2015).
460 However, Excel calculations ran relatively slowly (2 min per day) despite the low number of
461 simulations (250). It remains to program the calculations more effectively, run more simulations
462 (10000) and explore the sensitivity of the parameters. Finally, the numerical method presented here
463 should be compared to other recent approaches (e.g. Grace et al. 2015; Hall et al. 2015; Hall et al.
464 2016; Schindler et al. 2017; Appling et al. 2018), bearing in mind underlying assumptions (Demars et
465 al. 2015; Holtgrieve et al. 2016).

466

467 ## Hydrological connectivity

468 Here I linked stream metabolism with a hydrological model partitioning groundwater and soil water
469 sources. This opens a new avenue to link stream metabolism to catchment scale biogeochemical
470 models. It is also worth noting that the observed patterns in ER remained, even after assuming that
471 lateral inflows had no oxygen (C_g=0). This study is now questioning the recommended practice (e.g.
472 Demars et al. 2015) to select river reaches with as little lateral inflows as possible to avoid the
473 necessity to correct for lateral inflows and simplify the whole stream metabolism equation and
474 associated requirements (McCutchan et al. 1998). Selecting these reaches will prevent us from
475 observing the effect of lateral inflows, which provide the natural linkages between land, water and
476 the atmosphere.

477 Here, peak flows had a lasting effect on ER independently of the season. This can be explained by
478 the hydrological connectivity between the organic soil and stream water. When the soil was dry, as

indicated by low soil moisture at or below 0.5 m^3 m^{-3}, stream respiration was stable. ER increased with lateral hydrological connectivity. Under high stable flows, soil porewater was hydrologically connected to the stream and could represent a source of carbon boosting bacterial activity (e.g. Fiebig and Lock 1991; Fischer et al. 2002; Fasching et al. 2014; 2016; Stegen et al. 2016), particularly when water flows through the organic (O) soil horizon rich in organic carbon (see Table 1) and interact less with the mineral (B) soil horizon (Stutter et al. 2012; Raymond et al. 2016). ER decreased slowly following peak flows possibly because of a decrease in the rate of carbon supply with time. Yet it took weeks for ER to return back to stable rates after major peak flows, rather than days in previous studies (e.g. Roberts et al. 2007; O'Connor et al. 2012; Griffiths et al. 2013). This could be explained by high retention of labile DOC (polysaccharide, amino-acids) and nutrients in the hyporheic zone and its associated biofilm able to support fast metabolism for several weeks (Freeman and Lock 1995; Fiebig 1997; Fischer et al. 2002). The lower retention of nitrate may be compensated by groundwater supply (40-95% of stream stable water flows; Table 1). In this type of stream the zone of contact between soil water and hyporheic flow (e.g. Battin et al. 2003b; Stegen et al. 2016) may be more important than the contact zone between stream water and river bed, i.e. the transient storage of water (Manson et al. 2010). In other stream types, leaf fall and fine sediment supply were able to maintain high respiration rates for long period of time in relatively stable riverbeds (e.g. Roberts et al. 2007; Larsen and Harvey 2017).

Organic carbon cycling and fluxes

The uptake length of organic carbon (Sw_{OC}) was according to expectations from streams with similar discharge (Young and Huryn 1999), but varied by an order of magnitude with changes in hydrological connectivity. The mineralisation velocity ($v_{f\text{-}OC}$) was higher than expected from streams of similar size (Hall et al. 2016). Much of the net uptake and mineralisation observed in this study is likely from labile organic matter (e.g. Fiebig and Lock 1991; Fischer et al. 2002; Fellman et al. 2009; Fasching et

al. 2014; 2016; Drake et al. 2015; Stegen et al. 2016). The DOC at the outlet of the catchment has probably lost most of its rapid biodegradability potential and this may explain in part the extremely slow decomposition rate of recovered natural DOC by reverse osmosis in the Cairn Burn (Stutter et al. 2013) or lack of observed reactivity (e.g. Kothawala et al. 2015; Winterdahl et al. 2016). Further studies combining stream metabolism and DOC quality are required to make stronger inferences (e.g. Fuß et al. 2017; Hutchins et al. 2017), notably at the groundwater (or soil water) – stream water interface coupled with microbial ecology (e.g. Fasching et al. 2014; Fasching et al. 2016; Stegen et al. 2016).

Several studies have reported significant carbon losses in similar small streams (e.g. 12-18% in Dawson et al. 2001, 10-20% in Billett et al. 2006, 19-26% in Drake et al. 2015). Here I suggest that this could result from stream respiration alone accounting for 23±11% of the annual total inputs of DOC in a first order stream, assuming implicitly that sunlight and other potential processes did not play a significant role (see below). More DOC losses will occur downstream through the whole network (Raymond et al. 2016; Bertuzzo et al. 2017; Moody and Worrall 2017). The stream efficiency to mineralise carbon will be much lower under very high flows (not part of this study) where POC losses are likely to be significant contributors to the carbon flux.

Role of sunlight

In the experiments by Cory et al. (2014) photo-mineralisation and partial photo-oxidation or photo-stimulated bacterial respiration did not exceed 0.34 g C m^{-2} day^{-1} which is about 10% of the bacterial respiration of the present study. Since their experiment was designed to quantify processes in the water column, it excluded the dominant site of bacterial activity in streams (I-III order), i.e. benthic biofilm metabolism (e.g. Battin et al. 2003a). Cory et al. (2014) areal estimates of bacterial respiration for I-III order stream (0.03 g C m^{-2} day^{-1}) was similar to the respiration of the water column in our study derived from BOD_5 measurements (0.5 mg O_2 L^{-1}), but this represented only

about 1% of the bacterial respiration (HR) of the present study. Once hyporheic and surface benthic processes are included, light seems to play a relatively minor role in running headwaters.

Role of other processes

The calculations of the organic carbon ecosystem efficiency assumed that carbon inputs were equivalent to DOC mineralised and DOC flux at the stream outlet. This neglected the potential role of DOC flocculation, the release of organic carbon by autotrophs and bacterial production. The pool of benthic organic matter was small (<10 g C m^{-2}), but the benthic pool could be continuously replenished by flocculated DOC settling in the benthos. Kerner et al. (2003) showed that 7-25% of DOC could be flocculated over 10 days, however the DOC of the studied stream only had about an hour to flocculate and settle. So flocculation is unlikely to be important in this study. Gross primary production was small relative to heterotrophic respiration, so it is unlikely that autotrophic organic carbon could fuel bacterial activities to any great extent. Finally, if bacterial production (BP) is about 5-20% of heterotrophic respiration (HR), and HR was 36% and 22% of total organic carbon flux in the paired stream and ECN stream respectively under low flow conditions, then BP may assimilate 1-7% of the carbon flux. Altogether, it suggests that the assumptions were reasonable, although the calculated stream efficiency to mineralise organic carbon is best seen as a maximum.

Upscaling

While the estimates of reach scale metabolic rates, DOC flux and CO_2 efflux at the catchment outlet estimates were well constrained, upscaling metabolic rates (notably HR) to the full length of the

552 stream implicitly assumed spatial homogeneity of fluxes. This may not be the case (e.g. Dawson et al.
553 2001; Dawson et al. 2002), but at least the metabolic rates and hydrological behaviours were found
554 to be similar in two independent streams with significant lateral inflows and the upscaling was
555 limited to the same stream order. Further studies should explore the downstream effects through
556 the river network (e.g. Raymond et al. 2016; Bertuzzo et al. 2017; Moody and Worrall 2017; Ulseth
557 et al. 2018).

558 The annual total stream DOC flux represented about 1% of the land to atmosphere CO_2 flux
559 previously measured in our study catchments (Chapman and Thurlow 1996). This difference in
560 magnitude correspond to global C river fluxes relative to annual gross C fluxes between the
561 atmosphere and land (Dawson 2013). Nonetheless, the global annual riverine flux of organic C (0.26-
562 0.53 Pg C $year^{-1}$) to the oceans is comparable to the annual C sequestration in soil (0.4 Pg C $year^{-1}$),
563 suggesting that terrestrially- derived aquatic losses of organic C may contribute to regulating
564 changes in soil organic carbon storage (Dawson 2013).

565 The estimation of CO_2 gas exchange with the atmosphere within the studied reaches was well
566 constrained, but the concentration of CO_2 only reflected a short stream section (due to the high
567 reaeration rates) near the outlet and its determination by calculation was also relatively uncertain
568 (see Abril et al. 2015). The results may be more illustrative and should really be confirmed with
569 further spatial studies measuring directly the partial pressure of CO_2 by collecting headspace
570 samples for gas chromatography (e.g. Hope et al. 1995) or with sensor technology based on infra-red
571 gas analysis (e.g. Johnson et al. 2010). Nonetheless, the results suggested that about two-thirds of
572 the CO_2 degassing from streams was of terrestrial origin, and that in-stream biotic emissions (net
573 ecosystem production) contributed about one-third on average (excluding peak flow events),
574 perhaps a little higher than average values from continental studies (11% in Borges et al. 2015; 28%
575 in Hotchkiss et al. 2015).

576

Conclusions

There is fire under water: an average 23±11% of the dissolved organic carbon inputs from the land was burnt by benthic microbial metabolism within about an hour of transit time in small watersheds (about 1 km^2). Hydrological pulses stimulated in-stream respiration to the extent that the proportion of respired DOC to total DOC fluxes was similar under stable flows varying by an order of magnitude. Predicted hydrological changes under climate change (e.g. Schneider et al. 2013) could further shift the metabolic balance of streams towards heterotrophy and increase land derived CO_2 emissions from streams.

Acknowledgments

I dedicate this study to the late Julian J.C. Dawson. Great thanks to Carol Taylor and Helen Watson for managing the long-term monitoring, Yvonne Cook and Susan McIntyre for running water chemical analyses, Marc Stutter for providing particulate organic carbon data, Allan Wilson, Gordon Ewen, Richard Gwatkin for helping to set up the facilities at the Cairn Burn, Glensaugh farm manager Donald Barrie for helping in many ways, and Tony Edwards for mentoring in the early years. This study was funded by the Scottish Government Rural and Environmental Science and Analytical Services (RESAS), with additional funding support as part of the UK Environmental Change Network (ECN), and NERC Macronutrient Cycles Program. The writing up was partly funded by the Norwegian Institute for Water Research (NIVA). The author acknowledges the provision of data forming part of the UK ECN wide dataset, https://catalogue.ceh.ac.uk/documents/456c24dd-0fe8-46c0-8ba5-855c001bc05f. The author is grateful for the comments raised by two anonymous referees and the editors, Emily Bernhardt and Robert Howarth.

601 **References**

602 Abril, G. and others 2015. Technical Note: Large overestimation of pCO(2) calculated from pH and
603 alkalinity in acidic, organic-rich freshwaters. Biogeosciences **12:** 67-78.

604 Acuña, V., and K. Tockner. 2010. The effects of alterations in temperature and flow regime on
605 organic carbon dynamics in Mediterranean river networks. Global Change Biology **16:** 2638-
606 2650.

607 Appling, A. P., R. O. Hall Jr., C. B. Yackulic, and M. Arroita. 2018. Overcoming equifinality: leveraging
608 long time series for stream metabolism estimation. Journal of Geophysical Research:
609 Biogeosciences **123:** 624–645.

610 Battin, T. J. and others 2008. Biophysical controls on organic carbon fluxes in fluvial networks.
611 Nature Geoscience **1:** 95-100.

612 Battin, T. J., L. A. Kaplan, J. D. Newbold, and C. M. E. Hansen. 2003a. Contributions of microbial
613 biofilms to ecosystem processes in stream mesocosms. Nature **426:** 439-442.

614 Battin, T. J., L. A. Kaplan, J. D. Newbold, and S. P. Hendricks. 2003b. A mixing model analysis of
615 stream solute dynamics and the contribution of a hyporheic zone to ecosystem function.
616 Freshwater Biology **48:** 995-1014.

617 Battin, T. J., S. Luyssaert, L. A. Kaplan, A. K. Aufdenkampe, A. Richter, and L. J. Tranvik. 2009. The
618 boundless carbon cycle. Nature Geoscience **2:** 598-600.

619 Bauer, J. E., W. J. Cai, P. A. Raymond, T. S. Bianchi, C. S. Hopkinson, and P. A. G. Regnier. 2013. The
620 changing carbon cycle of the coastal ocean. Nature **504**: 61-70.

621 Beaulieu, J. J., C. P. Arango, D. A. Balz, and W. D. Shuster. 2013. Continuous monitoring reveals
622 multiple controls on ecosystem metabolism in a suburban stream. Freshwater Biology **58:**
623 918-937.

624 Bernhardt, E. S., J. R. Blaszczak, C. D. Ficken, M. L. Fork, K. E. Kaiser, and E. C. Seybold. 2017. Control
625 points in ecosystems: moving beyond the hot spot hot moment concept. Ecosystems **20:**
626 665-682.

627 Bernhardt, E. S. and others 2018. The metabolic regimes of flowing waters. Limnology and
628 Oceanography**:** doi: 10.1002/lno.10726.
629 Bertuzzo, E., A. M. Helton, R. O. Hall, and T. J. Battin. 2017. Scaling of dissolved organic carbon
630 removal in river networks. Adv. Water Resour. **110:** 136-146.
631 Besag. J., and P. Clifford. 1989. Generalized Monte Carlo significance tests. Biometrika **76**: 633–642.
632 Billett, M. F., C. M. Deacon, S. M. Palmer, J. J. C. Dawson, and D. Hope. 2006. Connecting organic
633 carbon in stream water and soils in a peatland catchment. Journal of Geophysical Research-
634 Biogeosciences **111:** G02010.
635 Borges, A. V. and others 2015. Globally significant greenhouse-gas emissions from African inland
636 waters. Nature Geoscience **8:** 637-642.
637 Brodie, R. S., and S. Hostetler. 2005. A review of techniques for analysing baseflow from stream
638 hydrographs. Proceedings of the NZHS-IAH-NZSSS 2005 Conference, Auckland, New Zealand.
639 Buckingham, S., E. Tipping, and J. Hamilton-Taylor. 2008. Concentrations and fluxes of dissolved
640 organic carbon in UK topsoils. Science of the Total Environment **407:** 460-470.
641 Butler, J. N. 1982. Carbon dioxide equilibria and their applications, 1st ed. Addison-Wesley, Reading.
642 Chapman, S. J., and M. Thurlow. 1996. The influence of climate on CO2 and CH4 emissions from
643 organic soils. Agricultural and Forest Meteorology **79:** 205-217.
644 Cole, J. J. and others 2007. Plumbing the global carbon cycle: Integrating inland waters into the
645 terrestrial carbon budget. Ecosystems **10:** 171-184.
646 Cooper, R., V. Thoss, and H. Watson. 2007. Factors influencing the release of dissolved organic
647 carbon and dissolved forms of nitrogen from a small upland headwater during autumn
648 runoff events. Hydrological Processes **21:** 622-633.
649 Cory, R. M., C. P. Ward, B. C. Crump, and G. W. Kling. 2014. Sunlight controls water column
650 processing of carbon in arctic fresh waters. Science **345:** 925-928.

651 Davidson, J. F., and E. J. Cullen. 1957. The determination of diffusion coefficients for sparingly
652 solubles gases in liquids. Transactions of the Institution of Chemical Engineers (Great Britain)
653 **35:** 51-60.
654 Dawson, J. J. C. 2013. Losses of soil carbon to the atmosphere via inland surface waters, p. DOI
655 10.1007/1978-1094-1007-6455-1002_1009. *In* R. Lal, et al [eds.], Ecosystem Services and
656 Carbon Sequestration in the Biosphere. Springer Science, Dordrecht
657 Dawson, J. J. C., C. Bakewell, and M. F. Billett. 2001. Is in-stream processing an important control on
658 spatial changes in carbon fluxes in headwater catchments? The Science of the Total
659 Environment **265:** 153-167.
660 Dawson, J. J. C., M. F. Billett, D. Hope, S. M. Palmer, and C. M. Deacon. 2004. Sources and sinks of
661 aquatic carbon in a peatland stream continuum. Biogeochemistry **70:** 71-92.
662 Dawson, J. J. C., M. F. Billett, C. Neal, and S. Hill. 2002. A comparison of particulate, dissolved and
663 gaseous carbon in two contrasting upland streams in the UK. Journal of Hydrology **257:** 226-
664 246.
665 Demars, B. O. L., and A. C. Edwards. 2007. Tissue nutrient concentrations in freshwater aquatic
666 macrophytes: high inter-taxon differences and low phenotypic response to nutrient supply.
667 Freshwater Biology **52:** 2073-2086.
668 Demars, B. O. L. and others 2016. Impact of warming on CO_2 emissions from streams countered by
669 aquatic photosynthesis. Nature Geoscience **9:** 758-761.
670 Demars, B. O. L., and J. R. Manson. 2013. Temperature dependence of stream aeration coefficients
671 and the effect of water turbulence: A critical review. Water Research **47:** 1-15.
672 Demars, B. O. L., J. R. Manson, J. S. Olafsson, G. M. Gislason, and N. Friberg. 2011a. Stream
673 hydraulics and temperature determine the metabolism of geothermal Icelandic streams.
674 Knowledge and Management of Aquatic Ecosystems **402:** 05.
675 Demars, B. O. L. and others 2011b. Temperature and the metabolic balance of streams. Freshwater
676 Biology **56:** 1106-1121.

677 Demars, B. O. L., J. Thompson, and J. R. Manson. 2015. Stream metabolism and the open diel oxygen
678 method: Principles, practice, and perspectives. Limnology and Oceanography-Methods **13:**
679 356-374.
680 Demars, B. O. L., J. Thompson, and J. R. Manson. 2017. Stream metabolism and the open diel oxygen
681 method: Principles, practice, and perspectives (vol 13, pg 356, 2015). Limnology and
682 Oceanography-Methods **15:** 219.
683 Drake, T. W., K. P. Wickland, R. G. M. Spencer, D. M. McKnight, and R. G. Striegl. 2015. Ancient low–
684 molecular-weight organic acids in permafrost fuel rapid carbon dioxide production upon
685 thaw. Proceedings of the National Academy of Sciences of the United States of America 112:
686 13946–13951.
687 Drake, T. W., P. A. Raymond, and R. G. M. Spencer. 2018. Terrestrial carbon inputs to inland waters:
688 A current synthesis of estimates and uncertainty. Limnology and Oceanography Letters **3**:
689 132-142.
690 Dunn, S. M. and others 2008. Interpretation of homogeneity in delta(18)O signatures of stream
691 water in a nested sub-catchment system in north-east Scotland. Hydrological Processes **22:**
692 4767-4782.
693 Dunn, S. M., S. I. Vinogradoff, G. J. P. Thornton, J. R. Bacon, M. C. Graham, and J. G. Farmer. 2006.
694 Quantifying hydrological budgets and pathways in a small upland catchment using a
695 combined modelling and tracer approach. Hydrological Processes **20:** 3049-3068.
696 Einarsdottir, K., M. B. Wallin, and S. Sobek. 2017. High terrestrial carbon load via groundwater to a
697 boreal lake dominated by surface water inflow. Journal of Geophysical Research-
698 Biogeosciences **122:** 15-29.
699 Fasching, C., B. Behounek, G. A. Singer, and T. J. Battin. 2014. Microbial degradation of terrigenous
700 dissolved organic matter and potential consequences for carbon cycling in brown-water
701 streams. Scientific Reports **4:** 4981.

Fasching, C., A. J. Ulseth, J. Schelker, G. Steniczka, and T. J. Battin. 2016. Hydrology controls dissolved organic matter export and composition in an Alpine stream and its hyporheic zone. Limnology and Oceanography **61:** 558-571.

Fellman, J. B., E. Hood, D. V. D'Amore, R. T. Edwards, and D. White. 2009. Seasonal changes in the chemical quality and biodegradability of dissolved organic matter exported from soils to streams in coastal temperate rainforest watersheds. Biogeochemistry **95:** 277-293.

Fiebig, D. M. 1997. Microbiological turnover of amino acids immobilized from groundwater discharged through hyporheic sediments. Limnology and Oceanography **42:** 763-768.

Fiebig, D. M., and M. A. Lock. 1991. Immobilization of dissolved organic matter from groundwater discharging through the stream bed. Freshwater Biology **26:** 45-55.

Findlay, S., and W. V. Sobczak. 1996. Variability in removal of dissolved organic carbon in hyporheic sediments. Journal of the North American Benthological Society **15:** 35-41.

Fischer, H., A. Sachse, C. E. W. Steinberg, and M. Pusch. 2002. Differential retention and utilization of dissolved organic carbon by bacteria in river sediments. Limnology and Oceanography **47:** 1702-1711.

Freeman, C., and M. A. Lock. 1995. The biofilm polysaccharide matrix: a buffer against changing organic substrate supply? Limnology & Oceanography **40:** 273-278.

Fuß, T., B. Behounek, A. J. Ulseth, and G. A. Singer. 2017. Land use controls stream ecosystem metabolism by shifting dissolved organic matter and nutrient regimes. Freshwater Biology **62:** 582-599.

Grace, M. R., D. P. Giling, S. Hladyz, V. Caron, R. M. Thompson, and R. Mac Nally. 2015. Fast processing of diel oxygen curves: Estimating stream metabolism with BASE (BAyesian Single-station Estimation). Limnology and Oceanography-Methods **13:** 103-114.

Griffiths, N. A. and others 2013. Agricultural land use alters the seasonality and magnitude of stream metabolism. Limnology and Oceanography **58:** 1513-1529.

727 Gustard, A., A. Bullock, and J. M. Dixon. 1992. Low flow estimation in the United Kingdom, p. 83.
728 Institute of Hydrology, Wallingford.
729 Hall, R. O., Jr., J. L. Tank, M. A. Baker, E. J. Rosi-Marshall, and E. R. Hotchkiss. 2016. Metabolism, gas
730 exchange, and carbon spiraling in rivers. Ecosystems **19:** 73-86.
731 Hall, R. O., Jr. and others 2015. Turbidity, light, temperature, and hydropeaking control primary
732 productivity in the Colorado River, Grand Canyon. Limnology and Oceanography **60:** 512-
733 526.
734 Hall, R. O., and H. L. Madinger. 2018. Use of argon to measure gas exchange in turbulent mountain
735 streams. Biogeosciences **15:** 3085–3092.
736 Hall, R. O., and J. L. Tank. 2005. Correcting whole-stream estimates of metabolism for groundwater
737 input. Limnology and Oceanography: Methods **3:** 222-229.
738 Hill Farming Research Organisation. 1983. Glensaugh Research Station. D & J Croal, Haddington.
739 Holtgrieve, G. W., D. E. Schindler, and K. Jankowski. 2016. Comment on Demars et al. 2015, "Stream
740 metabolism and the open diel oxygen method: Principles, practice, and perspectives".
741 Limnology and Oceanography-Methods **14:** 110-113.
742 Hope, D., J. J. C. Dawson, M. S. Cresser, and M. F. Billett. 1995. A method for measuring free CO_2 in
743 upland streamwater using headspace analysis. Journal of Hydrology **166:** 1-14.
744 Hope, D., S. M. Palmer, M. F. Billett, and J. J. C. Dawson. 2001. Carbon dioxide and methane evasion
745 from a temperate peatland stream. Limnology & Oceanography **46:** 847-857.
746 Hotchkiss, E. R. and others 2015. Sources of and processes controlling CO_2 emissions change with the
747 size of streams and rivers. Nature Geoscience **8:** 696-699.
748 Hutchins, R. H. S., P. Aukes, S. L. Schiff, T. Dittmar, Y. T. Prairie, and P. A. del Giorgio. 2017. The
749 optical, chemical, and molecular dissolved organic matter succession along a boreal soil-
750 stream-river continuum. Journal of Geophysical Research: Biogeosciences **122:** 2892–2908

751 Izagirre, O., U. Agirre, M. Bermejo, J. Pozo, and A. Elosegi. 2008. Environmental controls of whole-
752 stream metabolism identified from continuous monitoring of Basque streams. Journal of the
753 North American Benthological Society **27:** 252-268.
754 Johnson, M. S., M. F. Billett, K. J. Dinsmore, M. Wallin, K. E. Dyson, and R. S. Jassal. 2010. Direct and
755 continuous measurement of dissolved carbon dioxide in freshwater aquatic systems-method
756 and applications. Ecohydrology **3:** 68-78.
757 Kaplan, L. A., T. N. Wiegner, J. D. Newbold, P. H. Ostrom, and H. Gandhi. 2008. Untangling the
758 complex issue of dissolved organic carbon uptake: a stable isotope approach. Freshwater
759 Biology **53:** 855-864.
760 Kerner, M., H. Hohenberg, S. Ertl, M. Reckermann, and A. Spitzy. 2003. Self-organization of dissolved
761 organic matter to micelle-like microparticles in river water. Nature **422**: 150-154.
762 Kothawala, D. N. and others 2015. The relative influence of land cover, hydrology, and in-stream
763 processing on the composition of dissolved organic matter in boreal streams. Journal of
764 Geophysical Research-Biogeosciences **120:** 1491-1505.
765 Larsen, L. G., and J. W. Harvey. 2017. Disrupted carbon cycling in restored and unrestored urban
766 streams: Critical timescales and controls. Limnology and Oceanography **62:** S160-S182.
767 Manson, J. R., B. O. L. Demars, S. G. Wallis, and V. Mytnik. 2010. A combined computational and
768 experimental approach to quantifying habitat complexity in Scottish upland streams, p.
769 paper 191. Proceedings of Hydropredict' 2010, International Interdisciplinary Conference on
770 Predictions for Hydrology, Ecology and Water Resource Management. Czech Republic,
771 Prague.
772 McClain, M. E. and others 2003. Biogeochemical hot spots and hot moments at the interface of
773 terrestrial and aquatic ecosystems. Ecosystems **6:** 301-312.
774 McCutchan, J. H., and W. M. Lewis. 2006. Groundwater flux and open-channel estimation of stream
775 metabolism: response to Hall and Tank. Limnology and Oceanography-Methods **4:** 213-215.

McCutchan, J. H., W. M. Lewis, and I. J. F. Saunders. 1998. Uncertainty in the estimation of stream metabolism from open-channel oxygen concentrations. Journal of the North American Benthological Society **17:** 155-164.

Miller, J. D., and D. Hirst. 1998. Trends in concentrations of solutes in an upland catchment in Scotland. Science of the Total Environment **216:** 77-88.

Moody, C. S., and F. Worrall. 2017. Modeling rates of DOC degradation using DOM composition and hydroclimatic variables. Journal of Geophysical Research-Biogeosciences **122:** 1175-1191.

Neal, C. 1988. pCO2 variations in streamwaters draining an acidic and acid sensitive spruce forested catchment in Mid-Wales. The Science of the Total Environment **76:** 279-283.

Neal, C., W. A. House, and K. Down. 1998. An assessment of excess carbon dioxide partial pressures in natural waters based on pH and alkalinity measurements. The Science of the Total Environment **210/211:** 173-185.

Newbold, J. D., P. J. Mulholland, J. W. Elwood, and R. V. Oneill. 1982. Organic carbon spiralling in stream ecosystems. Oikos **38:** 266-272.

O'Connor, B. L., J. W. Harvey, and L. E. McPhillips. 2012. Thresholds of flow-induced bed disturbances and their effects on stream metabolism in an agricultural river. Water Resources Research **48:** W08504.

Odum, H. T. 1956. Primary production in flowing waters. Limnology and Oceanography **1:** 102-117.

Palmer, S. M., D. Hope, M. F. Billett, F. H. Dawson, and C. L. Bryant. 2001. Sources of organic and inorganic carbon in a headwater stream: evidence form carbon isotope studies. Biogeochemistry **52:** 321-338.

Raymond, P. A. and others 2013. Global carbon dioxide emissions from inland waters. Nature **503:** 355-359.

Raymond, P. A., J. E. Saiers, and W. V. Sobczak. 2016. Hydrological and biogeochemical controls on watershed dissolved organic matter transport: pulse-shunt concept. Ecology **97:** 5-16.

Reisinger, A. J., E. J. Rosi, H. A. Bechtold, T. R. Doody, S. S. Kaushal, and P. M. Groffman. 2017. Recovery and resilience of urban stream metabolism following Superstorm Sandy and other floods. Ecosphere **8:** e01776.

Roberts, B. J., P. J. Mulholland, and W. R. Hill. 2007. Multiple scales of temporal variability in ecosystem metabolism rates: Results from 2 years of continuous monitoring in a forested headwater stream. Ecosystems **10:** 588-606.

Roley, S. S., J. L. Tank, N. A. Griffiths, R. O. Hall, and R. T. Davis. 2014. The influence of floodplain restoration on whole-stream metabolism in an agricultural stream: insights from a 5-year continuous data set. Freshwater Science **33**:1043-1059.

Scharlemann, J. P. W., E. V. J. Tanner, R. Hiederer, and V. Kapos. 2014. Global soil carbon: understanding and managing the largest terrestrial carbon pool. Carbon Management **5:** 81-91.

Schindler, D. E., K. Jankowski, Z. T. A'Mar, and G. W. Holtgrieve. 2017. Two-stage metabolism inferred from diel oxygen dynamics in aquatic ecosystems. Ecosphere **8:** e01867.

Schneider, C., C. L. R. Laize, M. C. Acreman, and M. Florke. 2013. How will climate change modify river flow regimes in Europe? Hydrology and Earth System Sciences **17:** 325-339.

Simpson, G. L. 2016. permute: functions for generating restricted permutations of data. R package version 0.9-4. https://CRAN.R-project.org/package=permute

Standing Committee of Analysts. 1981. The determination of alkalinity and acidity in water. HMSO, London.

Stegen, J. C. and others 2016. Groundwater-surface water mixing shifts ecological assembly processes and stimulates organic carbon turnover. Nature Communications **7:** 11237.

Stimson, A. G., T. E. H. Allott, S. Boult, and M. G. Evans. 2017. Fluvial organic carbon composition and concentration variability within a peatland catchment-Implications for carbon cycling and water treatment. Hydrological Processes **31:** 4183-4194.

826 Stumm, W., and J. J. Morgan. 1981. Aquatic Chemistry. An introduction emphasizing chemical
827 equilibria in natural waters. Wiley Interscience, New York.
828 Stutter, M. I., S. M. Dunn, and D. G. Lumsdon. 2012. Dissolved organic carbon dynamics in a UK
829 podzolic moorland catchment: linking storm hydrochemistry, flow path analysis and sorption
830 experiments. Biogeosciences **9:** 2159-2175.
831 Stutter, M. I., D. G. Lumsdon, and A. P. Rowland. 2011. Three representative UK moorland soils show
832 differences in decadal release of dissolved organic carbon in response to environmental
833 change. Biogeosciences **8:** 3661-3675.
834 Stutter, M. I., S. Richards, and J. J. C. Dawson. 2013. Biodegradability of natural dissolved organic
835 matter collected from a UK moorland stream. Water Research **47:** 1169-1180.
836 ter Braak, C. J. F. 1990. Update notes: CANOCO version 3.10. statistical manual, Agricultural
837 Mathematics Group, Wageningen.
838 ter Braak, C. J. F., and P. Šmilauer. 2012. Canoco reference manual and user's guide: software for
839 ordination, version 5.0. Microcomputer Power, Ithaca, USA.
840 Uehlinger, U. 2000. Resistance and resilience of ecosystem metabolism in a flood-prone river
841 system. Freshwater Biology **45:** 319-332.
842 Uehlinger, U. 2006. Annual cycle and inter-annual variability of gross primary production and
843 ecosystem respiration in a floodprone river during a 15-year period. Freshwater Biology **51:**
844 938-950.
845 Ulseth, A. J., E. Bertuzzo, G. A. Singer, J. Schelker, and T. J. Battin. 2018. Climate-induced changes in
846 spring snowmelt impact ecosystem metabolism and carbon fluxes in an alpine stream
847 network. Ecosystems **21:** 373-390.
848 Williams, P. J. l. B., and P. A. del Giorgio. 2005. Respiration in aquatic ecosystems: history and
849 background, p. 1-17. *In* P. A. del Giorgio and P. J. l. B. Williams [eds.], Respiration in aquatic
850 ecosystems. Oxford University Press, Oxford.

Winterdahl, M., M. B. Wallin, R. H. Karlsen, H. Laudon, M. Oquist, and S. W. Lyon. 2016. Decoupling of carbon dioxide and dissolved organic carbon in boreal headwater streams. Journal of Geophysical Research-Biogeosciences **121:** 2630-2651.

Young, R. G., and A. D. Huryn. 1998. Comment: improvements to the diurnal upstream-downstream dissolved oxygen change technique for determining whole-stream metabolism in small streams. Canadian Journal of Fisheries and Aquatic Sciences **55:** 1784-1785.

Young, R. G., and A. D. Huryn. 1999. Effects of land use on stream metabolism and organic matter turnover. Ecological Application **9:** 1359-1376.

Zhang, J., P. D. Quay, and D. O. Wilbur. 1995. Carbon isotope fractionation during gas water exchange and dissolution of CO_2. Geochimica Et Cosmochimica Acta **59:** 107-114.

863 **Table 1.** Average inorganic nutrients and DOC concentrations (±sem) in groundwater from spring
864 samples scattered across the two catchments (2006), soil water from the humus iron podzol in the
865 organic horizon (10 cm) and subsoil (45 cm) at the ECN monitoring site (2007-2008), and stream
866 water at the outlets of Birnie ECN stream and Cairn Burn (2007-2008). n represents the number of
867 samples.

			NO_3-N	NH_4-N	PO_4-P	DOC
		n	µg N L^{-1}	µg N L^{-1}	µg P L^{-1}	mg C L^{-1}
groundwater	June	21	**363 ±90**	12 ±4	4 ±0.3	1.3 ±0.2
	November	13	**563 ±73**	13 ±5	7 ±1.0	8.0 ±3.0
soil water	10 cm depth	50	62 ±5	28 ±3	5 ±1.0	**23.4 ±1.1**
	45 cm depth	52	37 ±2	13 ±1	3 ±0.3	4.2 ±0.1
stream water	Birnie ECN	100	184 ±7	17 ±3	5 ±0.5	7.0 ±0.4
	Cairn	74	135 ±8	12 ±1	4 ±0.3	4.5 ±0.4

868

869

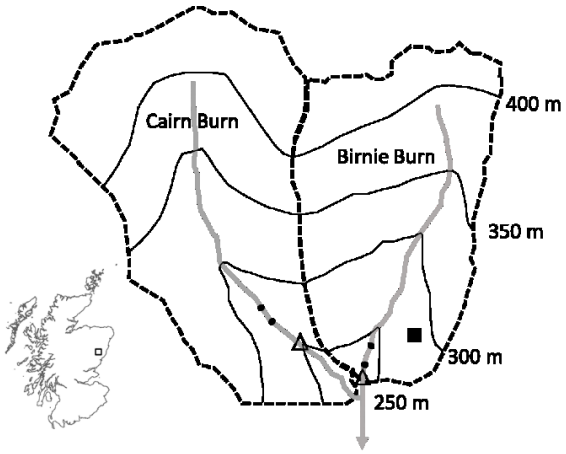

870

871 **Fig 1. Glensaugh research station: Birnie Burn is the Environmental Change Network (ECN) stream**
872 **and Cairn Burn the paired stream.** The symbols refer to flumes (open triangles), dissolved oxygen
873 stations (filled circles) and soil moisture instrumentation (filled square). The 50 m elevation contour
874 lines are indicated. The catchment area is 0.99 km^2 (0.90 km^2 at the flume) for Cairn Burn and 0.76
875 km^2 for Birnie Burn. Inset shows the location of Glensaugh in Scotland, UK.

876

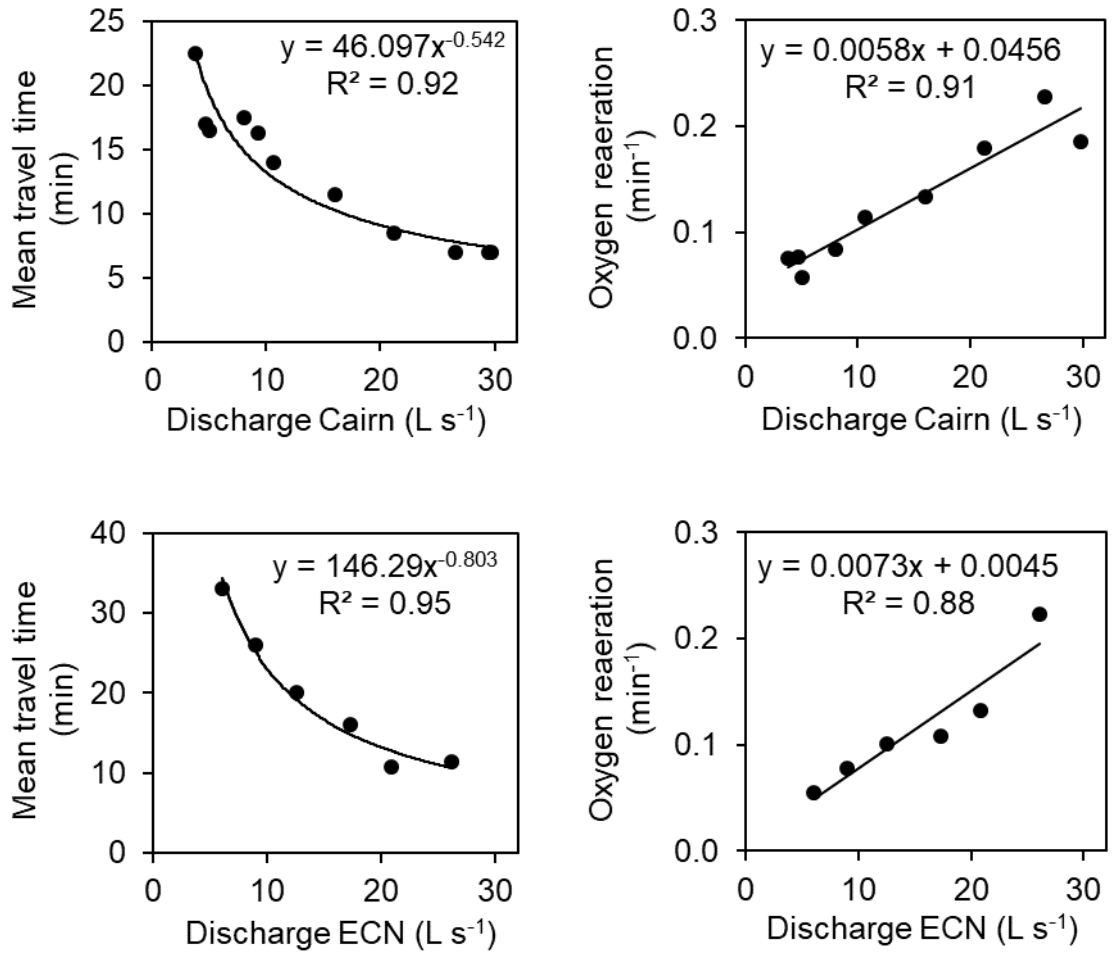

877

878

879

880 **Fig 2.** Mean travel time and oxygen reaeration coefficient as a function of discharge measured at the
881 flumes in the Cairn Burn (paired stream) and Birnie Burn ECN streams, top and bottom graphs
882 respectively.

883

884

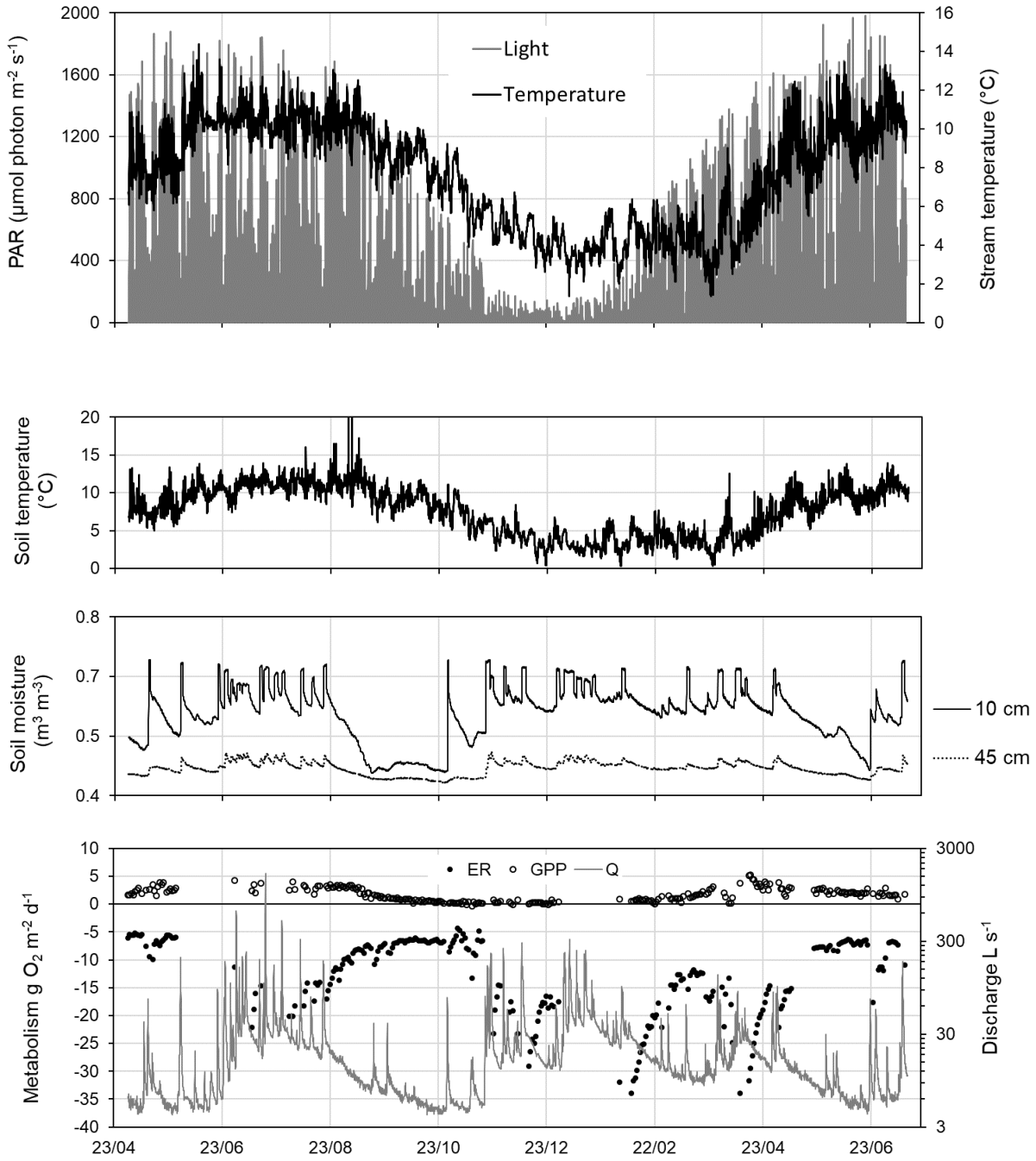

885

886

887

888

889 **Fig 3. Stimulation of ecosystem respiration following peak flows.** Continuous monitoring May 2007
890 – July 2008 of the paired stream Cairn Burn: (**a**) Photosynthetic active radiation (shaded area) and
891 stream water temperature (black line), (**b**) Soil temperature, (**c**) Soil moisture at the bottom of the
892 organic horizon (10 cm) and subsoil (45 cm), (**d**) metabolism with ecosystem respiration (negative
893 values, black filled circles) and gross primary production (positive values, open circles), discharge on
894 a log scale (grey line).

895

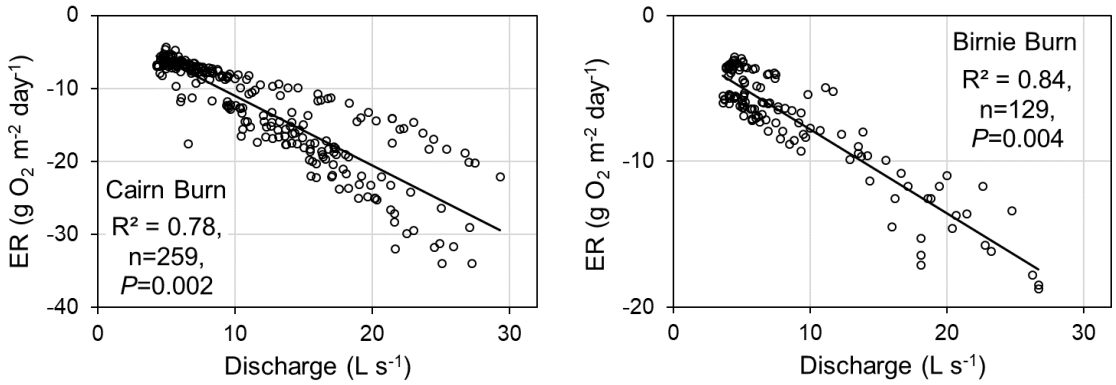

896

897 **Fig 4.** Ecosystem respiration (ER) increases with discharge in both streams (within low stable flow
898 conditions).

899

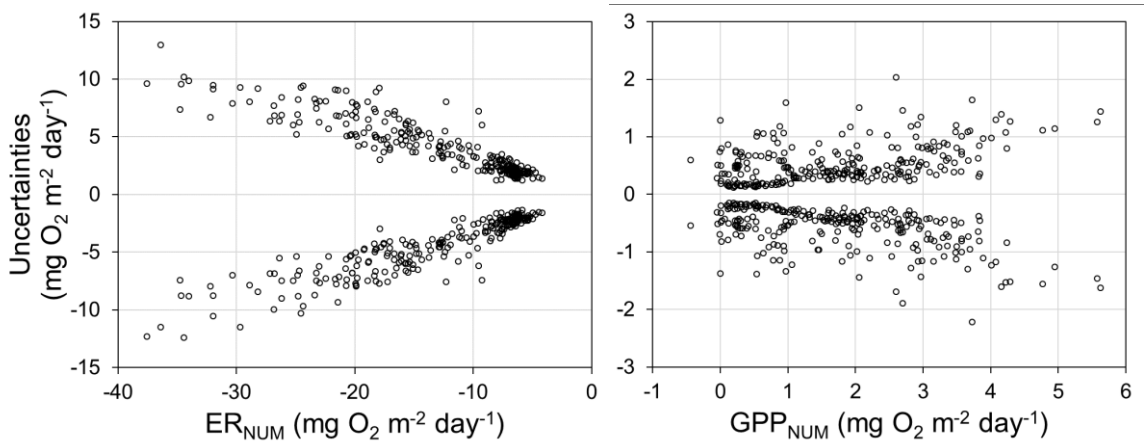

Fig. 5. Cairn Burn uncertainties (95% confidence interval) in daily ecosystem respiration (ER_{NUM}) and gross primary production (GPP_{NUM}) as a function of median daily ER_{NUM} and GPP_{NUM} determined numerically using Monte Carlo simulations. Uncertainties on the y axis represents 50^{th} – 97.5^{th} centiles (negative values) and 50^{th} – 2.5^{th} centiles (positive values).

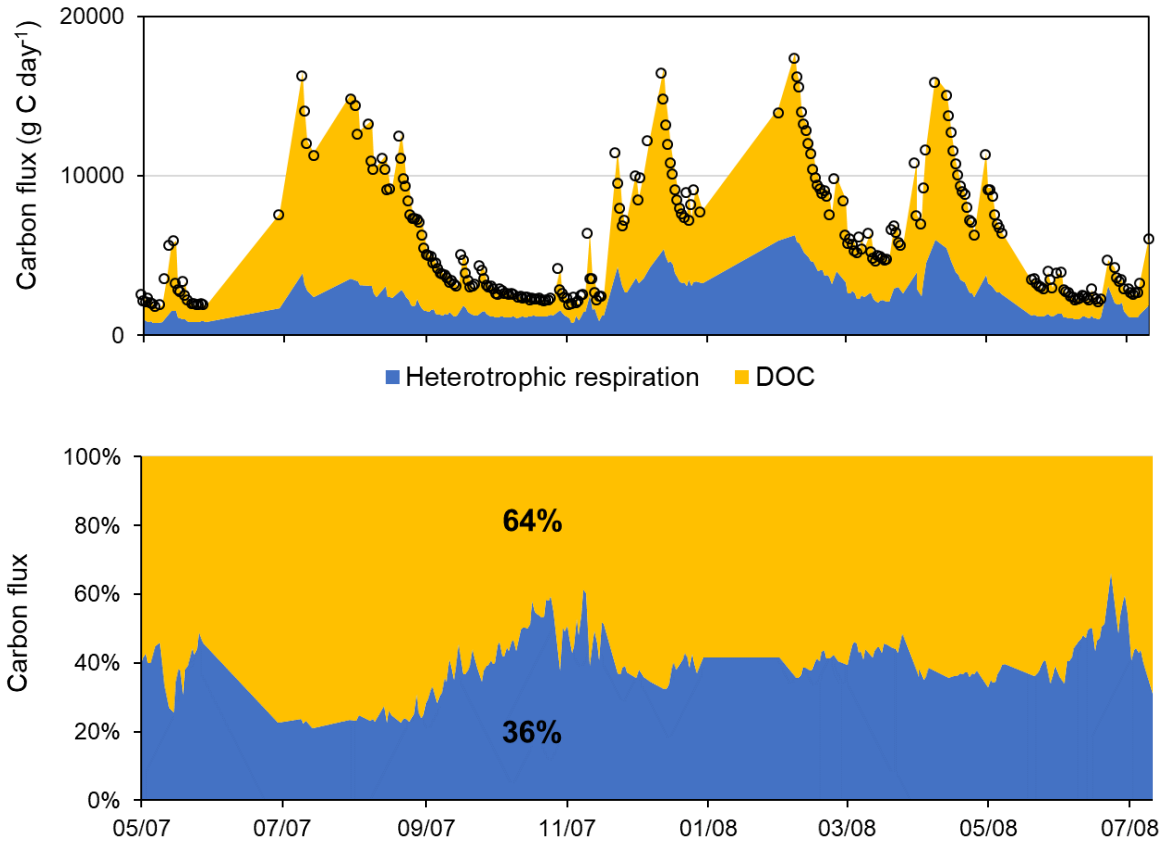

907

908

909 **Fig. 6** Organic carbon flux and proportion of dissolved organic carbon (DOC) removed by stream
910 respiration under low flow conditions (3-30 L s^{-1}) in a first order stream (Cairn Burn), May 2007 – July
911 2008. The dates for which stream respiration was estimated are indicated by open circles.

912 [colour online version]

913

914

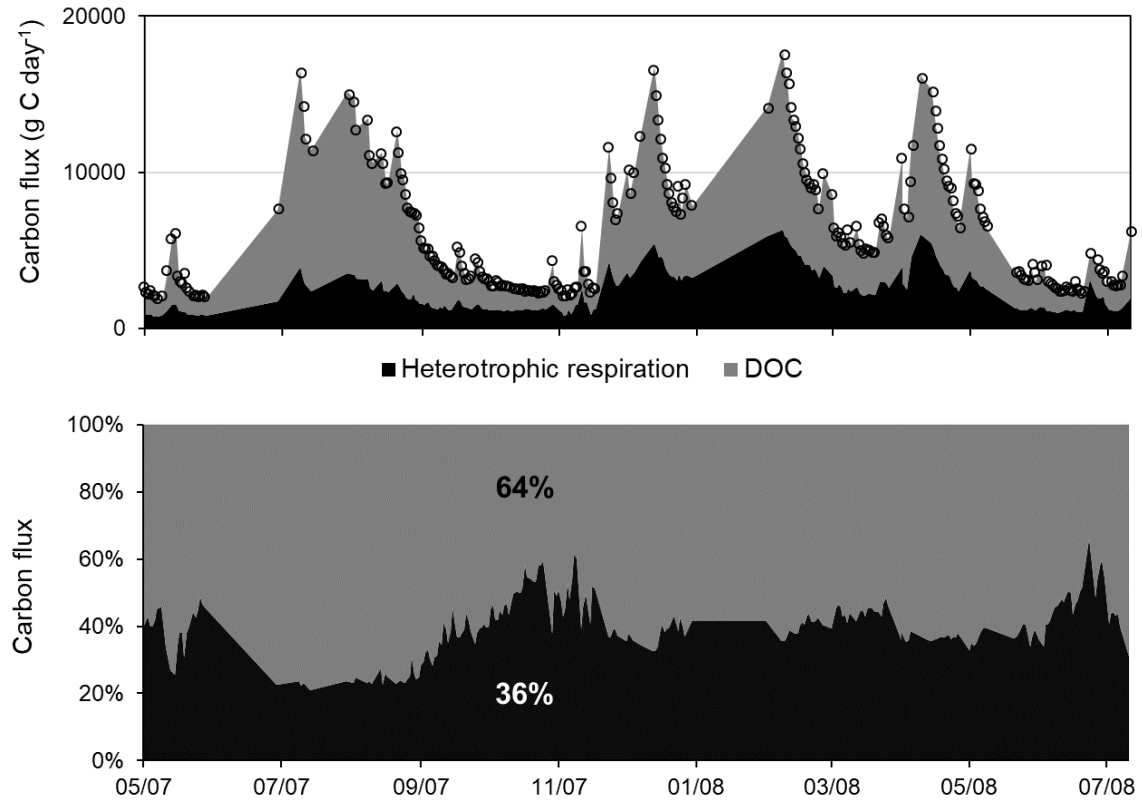

915

916

917 **Fig. 6 DOC flux curbed by in stream respiration.** Organic carbon flux and proportion of dissolved
918 organic carbon (DOC) removed by stream respiration under low flow conditions (3-30 L s^{-1}) in a first
919 order stream (Cairn Burn), May 2007 – July 2008. The dates for which stream respiration was
920 estimated are indicated by open circles.

921 [print black and white version]

922

923

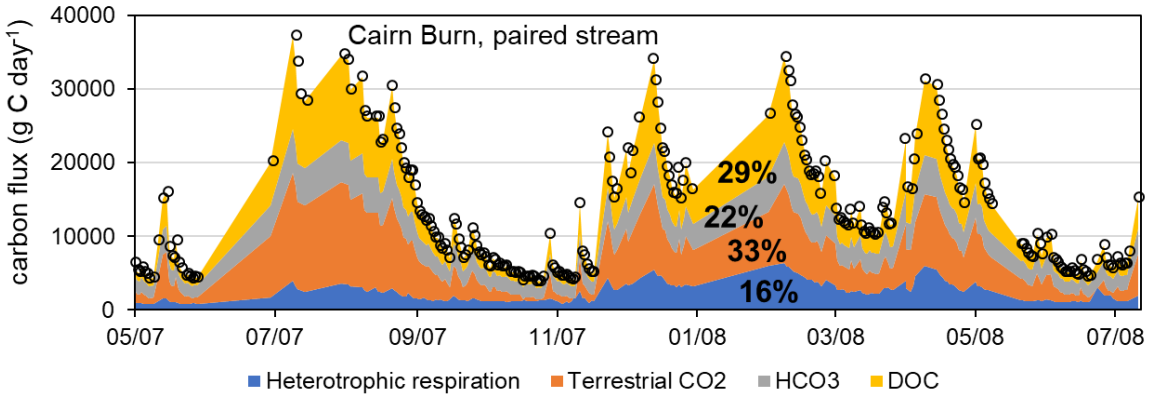

924

925 **Fig 7.** Total carbon flux from the Cairn Burn from May 2007 to July 2008 under low flow conditions
926 partitioned into four components: in-stream heterotrophic respiration, terrestrial CO_2 from
927 groundwater and sub-surface flows, bicarbonate and dissolved organic carbon at the outlet of the
928 catchments. The dates for which stream respiration was estimated are indicated by open circles.

929 [colour online version]

930

931

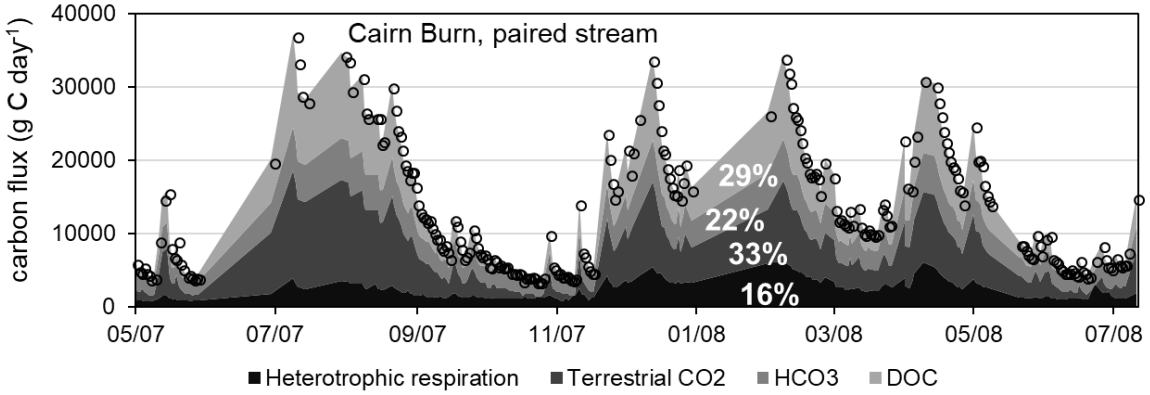

932

933 **Fig 7.** Total carbon flux from the Cairn Burn from May 2007 to July 2008 under low flow conditions
934 partitioned into four components: in-stream heterotrophic respiration, terrestrial CO_2 from
935 groundwater and sub-surface flows, bicarbonate and dissolved organic carbon at the outlet of the
936 catchments. The dates for which stream respiration was estimated are indicated by open circles.

937 [black and white print version]

938